HUNGARIAN JOURNAL OF
INDUSTRY AND CHEMISTRY
Vol. 54(1) pp. 1–12 (2026)
hjic.mk.uni-pannon.hu
DOI: 10.33927/hjic-2026-01

COMPARATIVE ADSORPTION STUDY OF CR(VI) AND MN(II) IONS USING RAW AND CHEMICALLY ACTIVATED POMEGRANATE PEEL-DERIVED CARBON

NIKHIL RAHUL DHONGDE[1,2*]; SHRAVAN KUMAR[2,3]; SAURABH MESHRAM[4]; SAMARJIT SINGH[4]; JAGAMOHAN MEHER[5]; SANDEEP DHARMADHIKARI[4]

1 Department of Chemistry, University of Saskatchewan, Saskatoon, Saskatchewan S7N 5C9, CANADA
2 Department of Chemical Engineering, Indian Institute of Technology Guwahati, Assam, 781039, INDIA
3 Department of Biochemical Engineering, Harcourt Butler Technical University, Kanpur, Uttar Pradesh, 208002, INDIA
4 Guru Ghasidas Vishwavidyalaya, Bilaspur, Chhattisgarh, 495009, INDIA
5 Krishi Vigyan Kendra, Kalahandi; Odisha University of Agriculture & Technology, Bhubaneswar, Odisha, 751003, INDIA

Chromium and Manganese ions are considered non-essential and highly toxic elements in drinking water. In this study, the adsorption of these ions from water was examined using pomegranate peel (PP) and activated carbon obtained from pomegranate peel (ACPP) as adsorbents. Pomegranate peel powder was chemically modified with phosphoric acid (H_3PO_4) to enhance the adsorption characteristics of activated carbon. A batch adsorption study was conducted to assess the effect of the solution's pH, temperature and contact time on adsorbent removal effectiveness. This adsorption isotherms study revealed that the adsorption of Mn(II) and Cr(VI) onto PP and ACPP follows the Langmuir isotherm with a correlation coefficient of more than 0.95. The maximum monolayer adsorption capacities of ACPP as well as PP were found to be 142.86 and 100.52 mg/g as well as 90.91 and 55.56 mg/g for Mn(II) and Cr(VI), respectively. The adsorption kinetics were investigated using the pseudo-first-order, pseudo-second-order and intraparticle diffusion models. The correlation coefficient indicated that the adsorption process adhered to pseudo-second-order kinetics. Moreover, the concurrence between the measured and computed values of q_e indicated a closely aligned adsorption equilibrium. The findings suggest that PP could be a cost-effective and promising adsorbent for effectively removing Cr(VI) and Mn(II).

Keywords: Cr(VI), Mn(II), pomegranate peel, activated carbon, adsorption isotherms, adsorption kinetics, adsorbent

1. Introduction

Rapid industrialization, unregulated urbanization and the unwise use of natural water resources have caused the contamination of water bodies and the mixing of heavy metals is a major culprit [1]-[3]. Characteristics of heavy metals such as their toxicity, non-biodegradability, carcinogenic nature and persistence in the environment cause more harmful effects to aquatic life [4]. The heavy metals ions Cr(VI) and Mn(II) are known to be highly toxic, moreover, bioaccumulate throughout the food chain and as a result of other human activities. These metals are discharged into the aqueous environment through several sources like textiles, metallurgical industries, microelectronics, fertilizers and pesticides. Furthermore, prolonged exposure to them or their intake in excess of the allowable limit of chromium metal ions is carcinogenic and may also cause several other health effects such as damage to the liver and kidneys [5]. In addition, the excessive intake of Mn(II) beyond its permissible limit causes neurological disorders [6]. The maximum allowed levels of Cr(VI) and Mn(II) in drinking water according to various organizations are presented in *Table 1*. According to the Bureau of Indian Standards (BIS), the permissible limits of Cr(VI) and Mn(II) in drinking water are 0.05 and 0.10 mg/L, respectively. Therefore, wastewater treatment to eliminate these metal ions is required before wastewater is discharged. Traditional techniques like precipitation, ion exchange, electrochemical treatment and membrane technologies are employed to eliminate heavy metal ions from wastewater. These methods have drawbacks such as their high costs, significant energy usage and the

Received: 30 July 2025; Revised: 6 Aug 2025;
Accepted: 18 Aug 2025
*Correspondence: nikhildhongde9194@gmail.com

Table 1: Overview of recommended values for samples of potable water

	Cr(VI) (mg/L)	Mn(II) (mg/L)
Bureau of Indian Standards (BIS), India	0.05	0.1
Environmental Quality Standards, European Union	0.05	0.001
World Health Organization (WHO)	0.05	0.4
U.S. Environmental Protection Agency (US EPA)	0.1	0.05

production of harmful sludge. Adsorption technologies based on natural biosorbents, on the other hand, provide a simple and cost-effective solution for wastewater treatment.

In recent years, several low-cost agriculture-based adsorbents such as datura stramonium fruit [7], caryota urens [8], wheat bran [9], sugarcane bagasse [10], peanut husk [11] and pressmud have been investigated for the elimination of Cr(VI) and Mn(II) metal ions. Rice husk-derived carbon quantum dots have the potential for cadmium absorption given their high solubility in water and the availability of oxygen-rich groups which act as binding sites with metallic substrates [12],[13]. These adsorbents are modified by chemical or physical activation methods to enhance adsorption. During chemical activation, a lignocellulosic precursor is blended with a substance that hinders tar formation. The activated carbon is generated through carbonization and subsequent washing. The chemical incorporated into the interior of the precursor undergoes reactions with the byproducts of its thermal decomposition, thereby reducing the emission of volatile substances and preventing particle contraction. The precursor is converted into carbon at a rapid rate by this method and once the chemical is removed following the heat treatment, a considerable level of porosity is generated [14].

Pomegranate or *Punica granatum* is known for being rich in phenolic compounds [15]. Producing approximately one million tons of pomegranate juice results in nearly nine million tons of peel and process waste. As of 2018, India was number one for pomegranate cultivation worldwide with around 234,000 hectares under cultivation and an annual production of 2.84 million metric tons [16]. Pomegranate peel (PP), an abundant agro-waste byproduct, has gained significant attention as a low-cost and eco-friendly adsorbent for removing various pollutants from aqueous solutions. Its rich composition of bioactive compounds and functional groups enhance its adsorption capacity. The effective utilization of waste PP for diverse applications is increasingly necessary to promote sustainability and reduce the amount of waste produced. PP powder, according to the pertinent literature, contains a significant number of functional groups, including hydroxyl and carboxylic groups, moreover, has demonstrated excellent efficacy in the elimination of ammonium ions. PP powder was used previously for the removal of ammonium [17], lead and copper [18], nickel [19] as well as phosphate [20].

Charuta Waghmare et al. [21] synthesized the phosphoric acid-treated PP adsorbent for the adsorption of methylene blue dye. Similarly, Shivali Singh Gaharwar et al. [22] reported the effective adsorption performance of phosphoric acid (H_3PO_4)-modified activated carbon synthesized using PP waste to remove protocatechuic acid. However, a comparative analysis of raw PP and chemically activated carbon synthesized using PP waste to remove the heavy metal ions Cr(VI) and Mn(II) from water has yet to be reported. Therefore, in this study, H_3PO_4 was used to chemically modify the adsorbent by synthesizing activated carbon using PP waste. The ability of PP to adsorb Cr(VI) and Mn(II) ions from a synthetic aqueous solution is studied in this work. Furthermore, efforts have been undertaken to transform this pomegranate peel waste into a chemically activated carbon adsorbent (ACPP) to remove Cr(VI) and Mn(II) from wastewater using H_3PO_4 acid. The effect of the solution's pH and contact time on metal ion elimination was studied. The examination of adsorption equilibrium data involved the utilization of Langmuir and Freundlich isotherm models along with pseudo-first-order (PFO), pseudo-second-order (PSO) and intraparticle diffusion kinetics models.

2. Experimental

2.1. Preparation of the stock solution

The synthetic solution of Cr(VI) and Mn(II) was prepared by using potassium dichromate ($K_2Cr_2O_7$) and manganese sulfate monohydrate ($MnSO_4*H_2O$). The study employed chemical reagents purchased from Loba Chemie, India. H_3PO_4 was purchased from Fisher Scientific, India.

2.2. Adsorbents

PP was sourced from the local market in Raipur, Chhattisgarh, India which was rinsed multiple times with distilled water before being dried for 15 h at 100 °C to eliminate moisture. The dried peel was crushed, sieved to achieve a particle size of 100 mesh and subsequently stored in silica gel desiccators. One portion of the raw pomegranate peel powder was used directly as the unmodified adsorbent. The other portion was chemically modified by being soaked in H_3PO_4 (85%) for 48 hours to enhance its adsorption properties. This modified peel powder was heated in a furnace for 1 h with a nitrogen (N_2) flow rate of 100 ml/min and a heating rate of 15 °C/min, reaching a temperature of 450 °C. The sample was then cooled to ambient temperature while maintaining the N_2 flow rate and rinsed with distilled water until the pH reached 6. It was then oven-dried for 12 h at 110 °C before being stored in desiccators for later

use. This second form of the adsorbent was labelled as ACPP. The activation procedure adopted in this experiment is consistent with that applied in previous studies [23],[24].

2.3. Batch adsorption studies

Batch adsorption tests were carried out by introducing a constant quantity of adsorbent into a 250 mL Erlenmeyer flask containing an aqueous solution with a known concentration of metal ions. The flask was then shaken at a consistent speed and temperature in an orbital shaker. The adsorbent was filtered out of the solution by centrifugation at 4000 rpm after a specified period of time. An Atomic Absorption Spectrophotometer (AAS) was used to ascertain the concentration of residual metal ions in the solution (ECIL, India). The effect of the solution's pH and adsorption time on the removal efficiency of metal ions as well as uptake capacity of adsorbents was also examined. The following equations were used to determine the metal ion uptake capacity and percent removal, respectively:

$$q_e = \frac{(C_0 - C_e)V}{m} \quad (1),$$

$$\%R = \frac{(C_0 - C_t)}{C_0} x\ 100 \quad (2),$$

where q_e represents the equilibrium adsorbent capacity in milligrams per gram, m stands for the mass of the adsorbent in grams and V denotes the volume of the solution in liters. The initial concentration, equilibrium concentration and concentration at any time t in the solution are represented by C_o, C_e and C_t, respectively. The percentage R represents the amount of heavy metal ions that were removed.

2.4. Characterization of the adsorbents

The microstructure and surface morphology of both PP and ACPP were examined before and after the adsorption of heavy metal ions using Field Emission Scanning Electron Microscopy (FESEM) at 15 kV conducted with a ZEISS EVO Series SEM. The surface area and pore volume were measured using the multipoint Brunauer, Emmett, and Teller (BET) method, which utilizes a fully automated Smart Sorb 93 analyzer and N_2 gas at 77 K under isothermal conditions. The structure and crystallinity of the synthesized adsorbents were determined through X-ray diffraction (XRD) analysis conducted on a PANalytical X'Pert Powder XRD multifunctional analyzer. To identify the functional groups present on the adsorbent surface, Fourier Transform Infrared Spectrometry (FTIR) was employed and the FTIR spectra of the adsorbents obtained using a Bruker Alpha spectrometer.

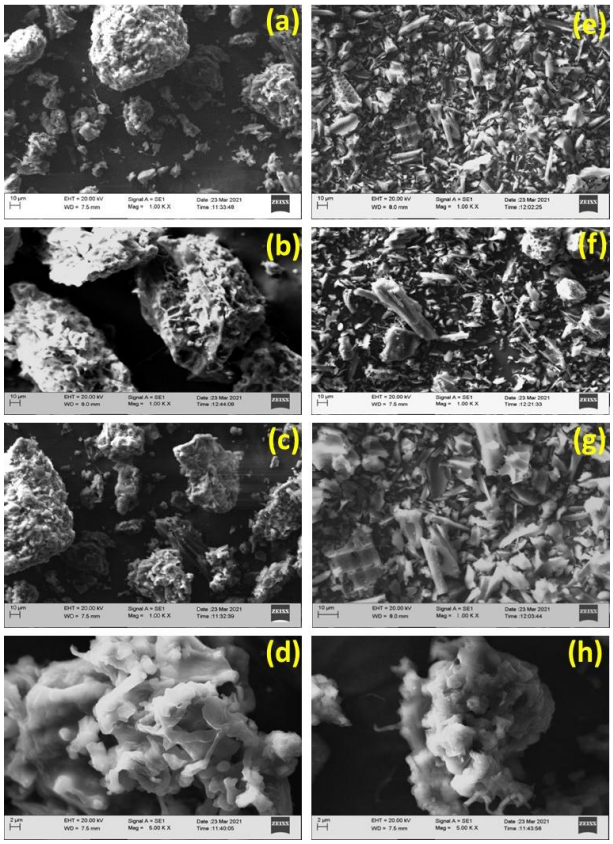

Figure 1: SEM image of unloaded PP (a,c), unloaded ACPP (b,d), Cr(VI) and Mn(II) loaded PP (e,g) and Cr(VI) and Mn(II)loaded ACPP (f,h)

3. Results and analysis

3.1. Characteristics of the adsorbent

To understand the adsorption behavior of Cr(VI) and Mn(II) over the derived adsorbent surface, the morphology of the adsorbents was analyzed using FESEM. The FESEM micrographs of PP before and after adsorption of the metal ions are shown in *Figure 1*. The FESEM micrographs of PP (*Figures 1a* and *1c*) indicate that the pores are not open, which is probably because of the existence of lignin, pectin and other viscous compounds that cause the fibers to stick together [25],[26]. It can be observed from *Figures 1b* and *1d* that the pores on the surface are open after the raw pomegranate peel had been activated by phosphoric acid, possibly due to the chemical treatment process removing volatile gases and viscous substances. The surface morphology of the adsorbent in *Figures 1a, 1b, 1c* and *1d* shows that it consists of irregular shapes, sizes, bends and broken edges on its surface. These surface characteristics allow the metal ions to diffuse from the solution onto the surface and into the pores. Furthermore, after the loading of metal ions, the surface morphology of the adsorbent became much smoother, indicating that adsorption had occurred. Similar results were reported in previous studies [27]-[29].

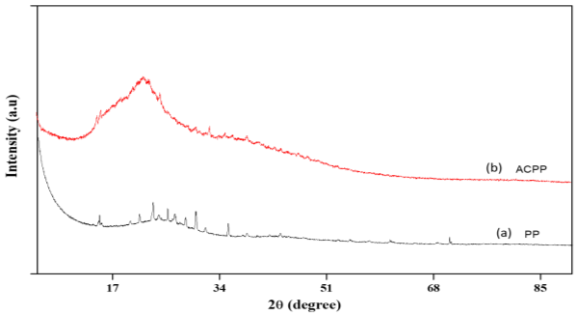

Figure 2: XRD spectra of (a) PP and (b) ACPP

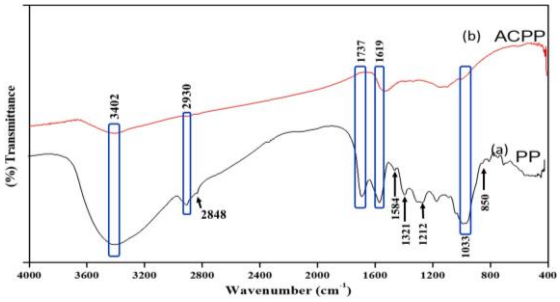

Figure 3: FTIR spectra of the adsorbents (a) PP and (b) ACPP

The XRD spectra of the synthesized PP and ACPP are presented in *Figure 2*. That of PP consists of sharp peaks at 14.72°, 21.10°, 23.10°, 30.06° and 35.20°, which indicates that PP is amorphous in nature. Jonghyun Choi et al. [30] also reported a similar trend according to XRD. In the XRD spectra of ACPP, sharp peaks are not found, indicating the absence of residual ash and impurities [31]. The peak at 25° of ACPP may be the result of diffraction by the (100) graphite plane [32], showing that the arrangement of its atoms or molecules is disordered. This can affect its physical and chemical properties, especially when applied for adsorption and catalysis.

The FTIR spectra of PP and ACPP are shown in *Figure 3*. In the spectrum of PP, the stretching vibrations of the hydroxyl groups of carboxylic acid, alcohols or phenol are represented by the peaks at the wavelengths of 3400 to 3300 cm^{-1}. The spectral peaks present at 2930.09 and 2848.42 cm^{-1} correspond to an aliphatic C-H group. The peaks observed at approximately 1737.63, 1619.20, 1584.49, 1321.09, 1212.87, 1033.19 and 850.00 cm^{-1} may correspond to C = O stretching, N–H bending, C–C in-ring stretching, N–O symmetric stretching, C–N stretching, =C–H bending and C–Cl stretching, respectively. On the other hand, the FTIR spectrum of the chemically activated ACPP adsorbent revealed the disappearance or significant reduction in intensity of several sharp peaks, indicating successful activation by H_3PO_4. This change can be attributed to the decomposition or transformation of specific functional groups during the activation process, altering the chemical structure and surface morphology of the adsorbent. The diminished or absence of peaks suggests the removal or modification of the original organic functional groups, confirming that the activation process effectively disrupted or restructured the surface chemistry. Additionally, the emergence or shifting of certain bands in the spectrum implies the formation of new functional groups or the enhancement of existing ones. Overall, the FTIR analysis indicates the presence of surface functionalities such as carboxylic (–COOH), hydroxyl (–OH) and amine ($–NH_2$) groups, which are essential for the adsorptive properties of the material.

3.2. Effect of pH on adsorption

The impact of the solution's pH on the adsorption of Mn(II) and Cr(VI) onto PP and ACPP was examined by tuning the pH within the range of 2 to 8 using standard hydrochloric acid (0.1 M) and sodium hydroxide (0.1 M) solutions. The initial concentrations of Mn(II) and Cr(VI) were set at 20 mg/L using a fixed adsorbent dosage of 0.2 g/L. The adsorption experiments were conducted at 298 K with continuous shaking at 200 rpm for a duration of 120 mins. All other process conditions such as the initial metal concentration, dosage, temperature, time and agitation speed were kept constant. The adsorption of Cr(VI) increased as the solution's pH decreased as illustrated in *Figure 4*. The maximum percentage removal of Cr(VI) was detected at a pH of 2 which is attributed to the presence of Cr(VI) ions in the solution such as $HCrO_4^-$, $Cr_2O_7^{2-}$ and CrO_4^{2-}, which alter the polarity of the adsorbent surface in response to the pH change in the solution. At lower pH values, the adsorbent surface becomes positively charged due to protonation, leading to electrostatic attraction between the chromium anions and the positively charged adsorbent surface. Conversely, at higher pH values, the prevalence of hydroxyl groups (OH-) increases, hindering the diffusion of Cr(VI) ions on the adsorbent surface, reducing the interaction between Cr(VI) and the adsorbent surface. Comparable findings were reported in studies on the adsorption of Cr(VI) by farmland soil [33] and by graphene/SiO_2 polypyrrole nanocomposites [34].

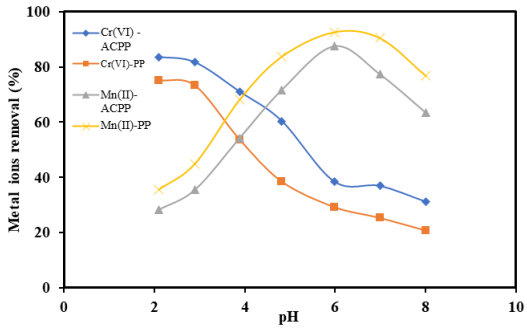

Figure 4: The influence of pH on the percentage removal of Cr(VI) and Mn(II) ions from the synthetic solution by the derived adsorbents
Conditions: Initial Cr(VI) and Mn(II) ion concentration = 20 mg/L, adsorbent dosage = 0.2 g/L, reaction time = 120 mins and temperature = 298 K

In the case of Mn(II) adsorption, as presented in *Figure 4*, the percentage removal of Mn(II) increased as the pH of the solution rose from 2 to 6. However, a decreasing trend in the percentage removal of Mn(II) is

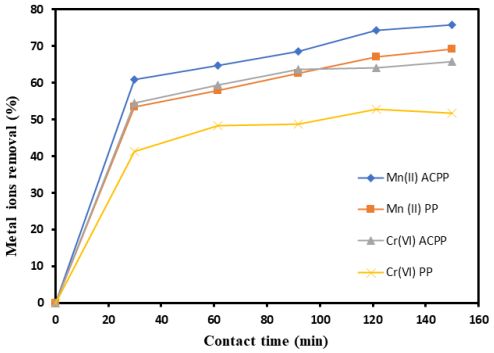

Figure 5: The effect of contact time on Cr(VI) and Mn(II) adsorption by PP and ACPP
Conditions: Initial Cr(VI) and Mn(II) ion concentration = 20 mg/L, adsorbent dosage = 0.2 g/L and temperature = 298 K

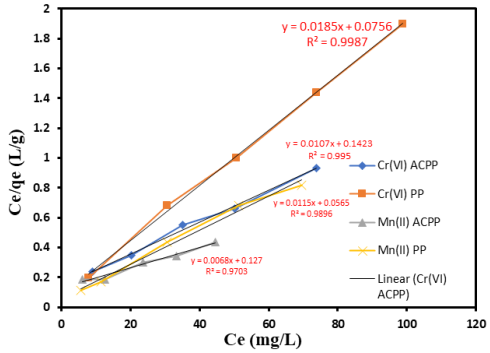

Figure 6: Langmuir isotherm adsorption curve of Cr(VI) and Mn(II) on PP and ACPP

observed beyond pH 6. The maximum percentage removal of Mn(II) was detected at pH 6. The reason for such a trend of Mn (II) adsorption is the hindrance in the diffusion of Mn(II) ions towards the binding site of the adsorbent as a result of the abundance of H^+ ions when the pH was less than 6. On the contrary, when the pH was greater than 6, Mn(II) ions precipitated as a result of the hydroxide anions forming a manganese hydroxide precipitate. Similar results were observed for Mn(II) adsorption onto activated carbon obtained from birbira leaves [35] and onto activated carbon synthesized from rice husk [36].

3.3. Effect of contact time on adsorption

In the batch mode adsorption process, a crucial factor is the contact time between the adsorbate and the adsorbent until an equilibrium is reached. The impact of the contact time on the percentage removal of Mn(II) and Cr(VI) by PP and ACPP is presented in *Figure 5* which indicates that the percentage removal of metal ions was notably high during the initial stages due to the plethora of active sites on the surfaces of the adsorbents, facilitating the rapid diffusion of metal ions onto them. However, following this initial rapid stage, the adsorption process of metal ions slowed down and after 120 mins no significant adsorption was observed. Consequently, 120 mins was selected as the ideal duration for subsequent studies. The same trends with regard to the rate of Mn(II) adsorption onto Zeolite Y were observed by Kwakye-Awuah et al. [37]. Finally, the metal ion percentage removal efficiencies of Mn(II)-PP and Cr(VI)-ACPP exhibited overlapping trends over time. However, after 120 mins, the removal efficiency of Mn(II) using PP was observed to be slightly lower than that of Cr(VI) using ACPP, which may be attributed to the enhanced surface area, porosity and presence of functional groups in ACPP that facilitate greater adsorption affinity and capacity for Cr(VI) ions. In contrast, the unmodified PP likely offers fewer active sites and weaker interactions with Mn(II) ions, resulting in a marginally reduced removal performance at equilibrium.

3.4. Adsorption isotherm study

To understand the distribution of solute between the solid and liquid phases, the conventional Langmuir and Freundlich isotherm models were employed to test the equilibrium data obtained using the adsorbents ACPP and PP. In this study, only the most appropriate isotherm model is examined in detail, while other models are not discussed further. Among the various options, the Langmuir and Freundlich isotherms demonstrated the best agreement with the experimental data across all concentrations as indicated by their high linear regression coefficients (R^2) of nearly 1.

Langmuir isotherm model

This model predicts the monolayer adsorption process.

$$\frac{C_e}{q_e} = \frac{1}{Q_0\, b} + \frac{C_e}{Q_0} \quad (3),$$

$$R_L = \frac{1}{1+bC_o} \quad (4),$$

where C_e represents the metal ion concentration at equilibrium (mg/L), q_e stands for the quantity of adsorbate absorbed per unit weight of adsorbent in milligrams per gram, Q_0 denotes the supreme adsorption capacity in mg/g and b refers to a Langmuir constant symbolizing bond energy.

The linear form of the model equation is presented in *Equation 3* [38].

The plot of C_e/q_e against C_e is linear as depicted in *Figure 6*. This linear graph was utilized to ascertain the Langmuir isotherm parameters outlined in *Table 2*. Additionally, the Langmuir isotherm yields a characteristic separation factor (R_L) also detailed in *Table 2*. R_L is an indicator of the adsorption process with $0<R_L<1$ signifying favorable adsorption, $R_L>1$ corresponding to unfavorable adsorption, $R_L=1$ indicating linear adsorption and $R_L=0$ representing an unalterable adsorption process. In this investigation, R_L values ranging from 0 to 1 were observed, confirming the favorable adsorption of the tested metal ions as noted by Koujalagi et al. [39].

Table 2: Langmuir and Freundlich isotherm model parameters for the adsorption of Mn(II) and Cr(VI) onto PP and ACPP

	Langmuir isotherm				Freundlich isotherm		
Metal ion onto Respective adsorbent	Q_m (mg g^{-1})	b (L g^{-1})	R^2	R_L	K_f (mg g^{-1}).(L $mg^{-1})^{1/n}$	n_f	R^2
Mn(II) onto PP	90.910	0.180	0.996	0.052	0.905	4.830	0.941
Mn(II) onto ACPP	142.860	0.058	0.970	0.146	18.110	2.164	0.926
Cr(VI) onto PP	55.560	0.428	0.998	0.022	34.197	11.230	0.908
Cr(VI) onto ACPP	100.000	0.062	0.997	0.137	19.186	2.976	0.979

Freundlich isotherm model

The Freundlich isotherm model was employed to analyze the multilayer adsorption process and the heterogeneous nature of adsorption sites [40]. The empirical model equation of the Freundlich isotherm model can be represented by this equation:

$$\log q_e = \log K_f + {}^1/_{n_f} \log C_e \quad (5),$$

where K_f and n represent the parameters of the Freundlich isotherm model corresponding to the adsorption energy and adsorption intensity, respectively.

The values of K_f and n provide insights into the heterogeneity and adsorption characteristics. The plot of log q_e against log C_e is linear, facilitating the evaluation of the dependent parameters K_f and $1/n$. The regression coefficient and parameters for both the Langmuir and Freundlich isotherm models are exhibited in *Table 2* which clearly show that the adsorption equilibrium data on the tested adsorbents align more closely with the Langmuir isotherm model than the Freundlich equivalent. This is evident from the higher R^2 values for the Langmuir isotherm model when compared to the Freundlich one. The fitting of the Langmuir isotherm model suggests that the adsorption of Cr(VI) and Mn(II) onto PP and ACPP is monolayer in nature. The adsorption capacity (Q_m) of ACPP for Mn(II) and Cr(VI) is 142.860 and 100.000 mg/g, respectively, indicating that ACPP is more effective in terms of adsorbing Mn(II).

This higher affinity can be attributed to the ion exchange and coordination mechanisms between Mn(II) ions and the surface functional groups of ACPP. Mn(II), a divalent cation, can interact strongly with adjacent hydroxyl and oxyl (carboxylate) groups on the ACPP surface, forming stable complexes through electron pair donation and establishing a coordination number of four. This interaction releases two hydrogen ions into the solution, facilitating an ion exchange mechanism. Additionally, the electrostatic attraction between the positively charged Mn(II) ions and negatively charged or electron-rich sites on ACPP enhances the adsorption efficiency. In contrast, Cr(VI), present as anionic species (e.g. $HCrO_4^-$, CrO_4^{2-}), may experience weaker electrostatic interactions or repulsion, resulting in poorer adsorption. Hence, the adsorbent ACPP performs better in terms of Mn(II) removal. The lack of a fit to the Freundlich isotherm model indicates that the adsorption of heavy metal ions onto PP and ACPP is not heterogeneous in nature.

3.5. Adsorption thermodynamics studies

In general, the wastewater treatment was conducted using an adsorption process within a temperature range of 300–350 K. Accordingly, in the present study, experimental investigations were carried out at 303, 323 and 343 K within this range. To assess the viability and nature of the adsorption process, thermodynamic variables, including changes in the standard Gibbs free energy ($\Delta G°$), enthalpy ($\Delta H°$) and entropy ($\Delta S°$), were determined using the equations below as outlined in the study by Chandraker et al. [38]:

$$\Delta G° = -RT \ln K_C \quad (6),$$

$$K_C = \frac{C_a}{C_e} \quad (7),$$

$$\ln K_C = -\frac{\Delta H°}{RT} + \frac{\Delta S°}{R} \quad (8),$$

where K_c denotes the thermodynamic equilibrium constant, R stands for the ideal gas constant, T represents the absolute temperature (K) and C_a refers to the solute concentration in the solid phase. Changes in the standard Gibbs free energy (kJ/mol), enthalpy (kJ/mol) and entropy (J/mol/K) are represented by $\Delta G°$, $\Delta H°$ and $\Delta S°$, respectively.

The values of $\Delta G°$ were obtained using *Equation 6* while those of $\Delta H°$ and $\Delta S°$ were calculated using the gradient and intercept of the plot ln K_c against $1/T$ shown in *Figure 7*. The values corresponding to $\Delta G°$, $\Delta H°$ and

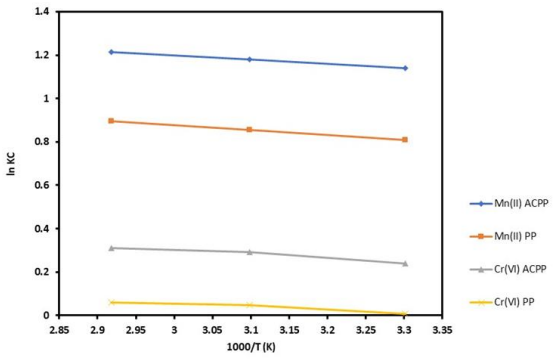

Figure 7: Thermodynamics curve for Cr(VI) and Mn(II) adsorption

Table 3: Thermodynamic parameters for the removal of metals ions by the adsorbents

Metal ion onto respective adsorbent	T (K)	Thermodynamic parameters $-\Delta G^{\circ}$ (kJ.mol^{-1})	ΔH° (kJ.mol^{-1})	ΔS° (kJ.mol^{-1}.K^{-1})
Mn(II) onto PP	303	2.8830	1.4258	0.0142
	323	3.1714		
	343	3.4517		
Mn(II) onto ACPP	303	2.0476	2.0751	0.0136
	323	2.3412		
	343	2.5910		
Cr(VI) onto PP	303	0.6420	1.5098	0.0071
	323	0.8131		
	343	0.9248		
Cr(VI) onto ACPP	303	0.0037	1.7434	0.0058
	323	0.1625		
	343	0.2325		

Table 4: Kinetics parameters for the pseudo-first-order, pseudo-second-order and intraparticle diffusion models

Sample	q_e (exp) (mg/g)	Pseudo-first-order			Pseudo-second-order			Intraparticle diffusion		
		k_1 (1/min)	q_e (cal) (mg/g)	R^2	k_2 (g/mg/min)	q_e (cal) (mg/g)	R^2	k_{id} mg/g/min^{½})	C (mg/g)	R^2
ACPP Cr(VI)	66.35	0.01	21.62	0.93	0.0014	71.43	0.99	1.83	45.07	0.93
PP Cr(VI)	52.35	0.03	36.47	0.94	0.0015	58.82	0.99	0.08	41.10	0.87
ACPP Mn(II)	75.68	0.02	44.66	0.85	0.0009	83.33	0.99	0.12	57.61	0.97
PP Mn(II)	69.27	0.02	36.89	0.88	0.0009	76.92	0.99	2.29	41.35	0.98

ΔS° are listed in *Table 3*. It was found that in all the experiments, the values of ΔH° were positive while those of ΔS° were negative, indicating that the adsorption process of Mn(II) and Cr(VI) onto PP and ACPP is endothermic, moreover, the entropy increased after adsorption. The negative ΔG° value suggests that the adsorption process is feasible and spontaneous.

3.6. Adsorption kinetic models

Understanding the adsorption mechanism involves fitting the batch adsorption data to kinetic model equations. To assess adsorption kinetics, the pseudo-first-order, pseudo-second-order and intraparticle diffusion model equations are utilized. The parameters for the kinetic models are presented in *Table 4*.

Pseudo-first-order model

According to this model, it is assumed that the adsorption of metal ions is directly proportional to the number of active sites available on the surface and can be expressed by the following equation [39]:

$$\log(q_e - q_t) = \log q_{e\,cal} - \frac{k_1}{2.030} t \qquad (9),$$

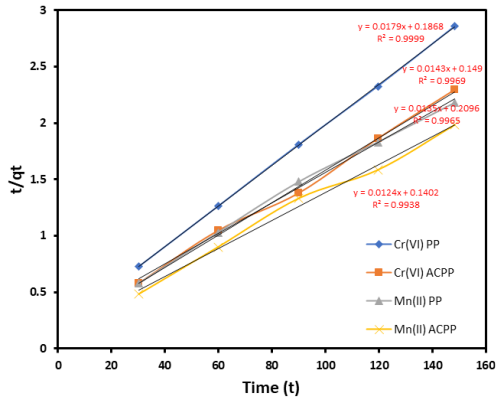

Figure 8: The pseudo-second-order kinetic models for Cr(VI) and Mn(II) on the tested adsorbents

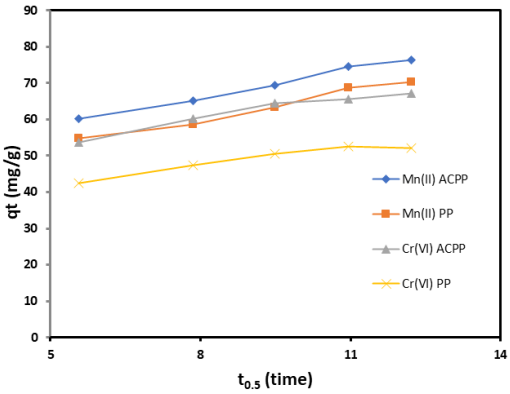

Figure 9: Intraparticle Diffusion Model for Cr(VI) and Mn(II) on the tested adsorbents

where k_1 represents the first-order rate constant (min^{-1}), q_e denotes the adsorbent uptake capacity at equilibrium and q_t stands for the adsorbent uptake capacity at time t.

Utilizing the plot of ln (q_e - q_t) against time (t), the parameters k_1 and q_e can be determined. However, the correlation coefficients observed for the pseudo-first-order kinetic model were low, moreover, notable disparities were evident between the experimental and theoretical parameters of equilibrium adsorption capacity (q_e). Consequently, it is indicated that the PFO model inadequately fits the experimental statistics.

Pseudo-second-order model

In this model, the adsorption rate is assumed to be proportional to the square of the difference between the amount of adsorbate adsorbed at equilibrium and that adsorbed at time t [41]. The linear form of this model is commonly expressed as given in the following equation:

$$\frac{t}{q_t} = \frac{1}{k_2 q_e^2} + \frac{t}{q_e} \quad (10),$$

where the rate constant for PSO adsorption is denoted by k_2 (g/mg min).

By plotting t/q_t against time (t), a linear relationship is obtained (*Figure 8*), moreover, the gradient and intercept of this line are utilized to compute the values of q_e and k_2. Among all the investigated kinetics for Mn(II) and Cr(VI) adsorption onto ACPP and PP surfaces, the PSO model exhibits the highest correlation coefficient. Additionally, the calculated q_e values closely match experimental values for PSO kinetics, indicating a high level of agreement with the experimental data. These findings suggest that the chemical sorption process, pertaining to the transfer or interchange of electrons between the solute and adsorbents, is the rate-controlling step.

Intraparticle diffusion model

The intraparticle diffusion model is commonly employed to characterize the adsorption process by distinguishing between internal diffusion within the adsorbent pores and external mass transfer resistance across the boundary layer surrounding the adsorbent particles. In order to determine the mechanism followed by the adsorption process, an intraparticle diffusion kinetic model is proposed by Weber and Morris [42]. The intraparticle diffusion can be expressed by this equation:

$$q_t = k_{id} t^{1/2} + c \quad (11),$$

where k_{id} represents the constant for the intraparticle diffusion kinetic model (mg/g.$min^{1/2}$) and c stands for the intercept, denoting the thickness of the boundary layer.

When c is large, the surface adsorption effect is more significant. This model assumes that intraparticle diffusion is a factor in the adsorption process. The plot of q_t against $t^{1/2}$ yields a linear graph (*Figure 9*) and its gradient is used to determine k_{id}. The linear plot originating from the origin signifies that the intraparticle diffusion process is not the exclusive rate-determining stage in the adsorption process, indicating that although intraparticle diffusion may play a role in the overall adsorption mechanism, additional factors such as surface adsorption, external diffusion or chemical interactions between the adsorbate and adsorbent are likely influential in regulating the rate of the process. The lack of deviation from the origin indicates the absence of substantial boundary layer resistance or external mass transfer constraints, suggesting that adsorption is regulated by a combination of various processes rather than solely by intraparticle diffusion. The results obtained in our investigations revealed the multifaceted nature regarding the plot of the intraparticle diffusion model, confirming that different adsorption mechanisms are involved in the adsorption process of the metal ions. The first stage of the curve suggests that the mechanism of metal ion adsorption is affected by outer surface sorption, while the second linear stage of the plot may be described by intraparticle diffusion. Moreover, intraparticle diffusion may be followed by more than one rate-controlling step because the linear plot deviated from the origin.

The adsorption of Cr(VI) and Mn(II) onto the adsorbents PP and ACPP transpires via monolayer adsorption, wherein the metal ions form a singular layer on the adsorbent surface. This process is governed by chemical interactions between metal ions and surface functional groups, including carboxylic (-COOH) and hydroxyl (-OH) groups, which are recognized for their ability to bond with metal ions via coordination and ion

exchange. The existence of these functional groups improves the adsorbent capacity to eliminate heavy metal ions by offering active sites for adsorption.

4. Discussion

The adsorption of Cr(VI) and Mn(II) onto the adsorbent PP/ACPP is highly dependent on the physicochemical properties of the adsorbent, particularly the surface functionalities and pore structure. FTIR analysis indicates the involvement of surface oxygen-containing groups such as hydroxyl, carboxyl and carbonyl moieties in the binding process. These groups can interact with metal ions through complexation and electrostatic attraction. In the case of Cr(VI), which exists primarily in the form of dichromate ($Cr_2O_7^{2-}$) or chromate (CrO_4^{2-}) at neutral to alkaline pHs, the negative charge facilitates strong interactions with positively charged protonated functional groups on the adsorbent surface. Mn(II), being a divalent cation, also exhibits strong affinity through ion exchange and complexation with electron-donating groups. The surface area and mesoporous structure of the activated PP/ACPP enhance the availability of these functional sites, further improving the adsorption capacity.

In addition to surface interactions, the role of redox processes in the adsorption mechanism cannot be overlooked, especially for Cr(VI), which undergoes reduction to the less toxic Cr(III) form during adsorption. This reduction is likely facilitated by electron-rich sites on the adsorbent surface such as phenolic or carbonyl groups which donate electrons to Cr(VI), resulting in its simultaneous reduction and adsorption. Thermodynamic parameters support this chemisorption process as indicated by the positive $\Delta H°$ values (endothermic nature) and negative $\Delta G°$ values, suggesting a spontaneous and favorable process. The increase in entropy ($\Delta S°$) implies enhanced randomness at the solid-liquid interface, likely due to the displacement of water molecules and reorganization of surface-bound ions during metal binding. The deviation of the intraparticle diffusion model from the origin and its multilinear profile indicate that adsorption is governed by multiple steps, including film diffusion, pore diffusion and surface adsorption, which occur sequentially or simultaneously.

Furthermore, the presence of oxygenated functional groups on the PP/ACPP adsorbent surface contributes significantly to Mn(II) adsorption by facilitating surface complexation, which is essential for the subsequent oxidation of Mn(II) to Mn(IV) species under ambient conditions. This catalytic role of the adsorbent underscores its multifunctionality that is adsorption coupled with redox transformation. For practical applications, the stability and regeneration of the adsorbent PP/ACPP are crucial. Batch and column studies must be integrated to evaluate breakthrough curves and determine adsorbent exhaustion points, which directly impact process scalability. The development of this low-cost, biowaste-derived adsorbent not only aligns with the principles of green chemistry but also offers a sustainable pathway for the removal of heavy metal ions in real-world wastewater systems. Comprehensive mechanical and economic evaluations will be required to validate its industrial applicability, ensuring a balance between efficiency, durability and operational costs.

Desorption studies are essential to evaluate the reproducibility of the performance of the adsorbent PP/ACPP, ensuring consistent behavior across multiple adsorption–desorption cycles. To comprehensively assess the applicability of this material in real-world scenarios, future research should incorporate validation using both batch and column methodologies, which simulate different operational conditions in wastewater treatment systems. Additionally, in-depth economic evaluations are necessary to determine the feasibility of scaling up the adsorption process for industrial wastewater treatment applications.

5. Conclusions

In this study, raw pomegranate peel and activated carbon from pomegranate peel through chemical activation with H_3PO_4 were prepared. To understand the adsorption mechanism, the adsorbents were characterized physico-chemically using SEM, XRD and FTIR analysis. It was found that the porous structure and pore volume of the raw PP increased after activation. The structure of PP was found to be crystalline and that of ACPP amorphous from XRD spectra. Surface functional groups of PP changed after activation by ACPP. The BET surface area of ACPP is larger than PP. The potential and applicability of PP and ACPP in the elimination of Cr(VI) and Mn (II) from aqueous solutions were studied. By examining the influence of contact duration, temperature and pH, it was demonstrated that the adsorption of Cr(VI) and Mn(II) onto the examined adsorbents closely followed the Langmuir isotherm and adhered to the pseudo-second-order kinetic model. This suggests that the adsorption process is influenced by these factors and that the adsorption sites on the adsorbent are homogeneously distributed with the rate of adsorption being governed by the interaction between the adsorbate and adsorbent surface. The optimal adsorption capacities of PP and ACPP were found to be 55.56 and 100.00 mg/g for Cr(IV) but 90.91 and 142.86 mg/g for Mn(II), respectively. Thermodynamic studies showed that the adsorption reaction is instantaneous, endothermic and random in nature on the adsorbent surface. Furthermore, it is observed from this investigation that the adsorbent ACPP exhibited a good degree of potential for the elimination of Mn(II) and Cr(VI) from aqueous solutions. Future research could explore the development of advanced activation methods to enhance the adsorption efficiency of ACPP for a wider range of pollutants, including emerging contaminants. Technically, scaling up the production of ACPP for industrial wastewater treatment applications could lead to cost-effective solutions for the large-scale removal of heavy metal ions like Cr(VI) and Mn(II). To maximize the utility of these materials, future research should focus

on optimizing activation methods for specific pollutants such as heavy metal ions, dyes and pharmaceuticals. Furthermore, these adsorbents could be effectively employed in decentralized water treatment systems, especially in rural or resource-limited areas. Their integration into filtration units for household water purification, wastewater treatment plants or even industrial effluent management presents promising practical applications. Additionally, investigating the regeneration and reusability of ACPP would improve its economic viability and sustainability in continuous industrial processes.

Acknowledgements

The authors are thankful to Guru Ghasidas Vishwavidyalaya (Bilaspur, Chhattisgarh, India) and the Department of Chemical Engineering at the Indian Institute of Technology Guwahati in Assam, India for providing the research facilities.

REFERENCES

[1] Kamalanathan, S.; Amran, F.; Zaini, M.A.A.: Oxidized mangosteen peel-derived hydrochar for the removal of methylene blue, *Hung. J. Ind. Chem.*, 2025, **53**(1), 1–7, DOI: 10.33927/hjic-2025-01

[2] Dutta, A.; Kundu, D.; Sharma, S.; Silvester, D.S.; Banerjee, T.: Investigating the electrochemical properties of ionic-liquid-mediated inorganic eutectogels derived from carboxylic-acid-based hydrophobic natural deep eutectic solvents, *J. Solut. Chem.*, 2025, **54**(9), 1210–1225, DOI: 10.1007/s10953-025-01471-2

[3] Dhongde, V.; Velpandian, M.; Haider, M.A.; Basu, S.: A $Sr_2CoNbO_{6-\delta}$@$Sm_{0.2}Ce_{0.8}O_{2-\delta}$ nanofiber composite as cathode accelerates oxygen reduction reaction for IT-SOFC, *ECS Trans.*, 2023, **111**(6), 2271–2276, DOI: 10.1149/11106.2271ecst

[4] Abdullah, T.A.; Al-Obaidi, Q.; Abdulla, T.A.; Rasheed, R.T.; Al-Azawi, K.; Meharban, F.: A critical review of the photocatalytic degradation of pharmaceutical residues by a TiO2-based photocatalyst, *Hung. J. Ind. Chem.*, 2024, **51**(2), 65–75, DOI: 10.33927/hjic-2023-20

[5] Kumar, S.; Narayanasamy, S.; Venkatesh, R.P.: Removal of Cr(VI) from synthetic solutions using water caltrop shell as a low-cost biosorbent, *Sep. Sci. Technol.*, 2019, **54**(17), 2783–2799, DOI: 10.1080/01496395.2018.1560333

[6] Adeogun, A.I.; Idowu, M.A.; Ofudje, A.E.; Kareem S.O.; Ahmed, S.A.: Comparative biosorption of Mn(II) and Pb(II) ions on raw and oxalic acid modified maize husk: kinetic, thermodynamic and isothermal studies, *Appl. Water Sci.*, 2013, **3**(1), 167–179, DOI: 10.1007/s13201-012-0070-1

[7] Kumar, S.; Shahnaz, T.; Selvaraju, N.; Rajaraman, P.V.: Kinetic and thermodynamic studies on biosorption of Cr(VI) on raw and chemically modified *Datura stramonium* fruit, *Environ. Monit. Assess.*, 2020, **192**(4), 248, DOI: 10.1007/s10661-020-8181-x

[8] Rangabhashiyam, S.; Selvaraju, N.: Evaluation of the biosorption potential of a novel *Caryota urens* inflorescence waste biomass for the removal of hexavalent chromium from aqueous solutions, *J. Taiwan Inst. Chem. Eng.*, 2015, **47**, 59–70, DOI: 10.1016/j.jtice.2014.09.034

[9] Nameni, M.; Alavi Moghadam, M.R.; Arami, M.: Adsorption of hexavalent chromium from aqueous solutions by wheat bran, *Int. J. Environ. Sci. Technol.*, 2008, **5**(2), 161–168, DOI: 10.1007/BF03326009

[10] Carvalho, J.T.T.; Milani, P.A.; Consonni, J.L.; Labuto, G.; Carrilho, E.N.V.M.: Nanomodified sugarcane bagasse biosorbent: synthesis, characterization, and application for Cu(II) removal from aqueous medium, *Environ. Sci. Pollut. Res.*, 2021, **28**(19), 24744–24755, DOI: 10.1007/s11356-020-11345-3

[11] Zaini, H.; Sami, M.; Arifin, R.: Activated variation of adsorbent and variation of contact time effects on manganese (II) in groundwater by column system using peanut shell as bioadsorbent, *IOP Conf. Ser. Mater. Sci. Eng.*, 2019, **536**(1), 012092, DOI: 10.1088/1757-899X/536/1/012092

[12] Wang, W.; Wang, Z.; Liu, J.; Peng, Y.; Yu, X.; Wang, W.; Zhang, Z.; Sun, L.: One-pot facile synthesis of graphene quantum dots from rice husks for Fe^{3+} sensing, *Ind. Eng. Chem. Res.*, 2018, **57**(28), 9144–9150, DOI: 10.1021/acs.iecr.8b00913

[13] Dhongde, N.R.; Das, N.K.; Banerjee, T.; Rajaraman, P.V.: Synthesis of carbon quantum dots from rice husk for anti-corrosive coating applications: Experimental and theoretical investigations, *Ind. Crops. Prod.*, 2024, **212**, 118329, DOI: 10.1016/j.indcrop.2024.118329

[14] Kang, Y.-H.; Shiue, A.; Hu, S.-C.; Huang, C.-Y.; Chen, H.-T.: Using phosphoric acid-impregnated activated carbon to improve the efficiency of chemical filters for the removal of airborne molecular contaminants (AMCs) in the make-up air unit (MAU) of a cleanroom, *Build. Environ.*, 2010, **45**(4), 929–935, DOI: 10.1016/j.buildenv.2009.09.012

[15] Gaharwar, S.S.; Kumar, A.; Mandavgane, S.A.; Rahagude, R.; Gokhale, S.; Yadav, K.; Borua, A.P.: Valorization of *Punica granatum* (pomegranate) peels: a case study of circular bioeconomy, *Biomass Convers. Biorefin.*, 2024, **14**(6), 7707–7724, DOI: 10.1007/s13399-022-02744-2

[16] Singh, J.; Kaur, H.P.; Verma, A.; Chahal, A.S.; Jajoria, K.; Rasane, P.; Kaur, S.; Gunjal, M.; Ercisli, S.; Choudhary, R.; Bozhuyuk, M.R.; Sakar, E.; Karatas, N.; Durul, M.S.: Pomegranate peel phytochemistry, pharmacological properties, methods of extraction, and its application: A comprehensive review, *ACS Omega*, 2023, **8**(39), 35452–35469, DOI: 10.1021/acsomega.3c02586

[17] Bellahsen, N.; Varga, G.; Halyag, N.; Kertész, S.; Tombácz, E.; Hodúr, C.: Pomegranate peel as a new low-cost adsorbent for ammonium removal, *Int. J. Environ. Sci. Technol.*, 2021, **18**(3), 711–722, DOI: 10.1007/s13762-020-02863-1

[18] Ben-Ali, S.: Application of raw and modified pomegranate peel for wastewater treatment: A literature overview and analysis, *Int. J. Chem. Eng.*, 2021, **2021**(1), 8840907, DOI: 10.1155/2021/8840907

[19] Khawaja, M.; Mubarak, S.; Zia-Ur-rehman, M.; Kazi, A.A.; Hamid, A.: Adsorption studies of pomegranate peel activated charcoal for nickel (II) ion, *J. Chil. Chem. Soc.*, 2015, **60**(4), 2642–2645, DOI: 10.4067/S0717-97072015000400003

[20] Bellahsen, N.; Kakuk, B.; Beszédes, S.; Bagi, Z.; Halyag, N.; Gyulavári, T.; Kertész, S.; El Amarti, A.; Tombácz, E.; Hodúr, C.: Iron-loaded pomegranate peel as a bio-adsorbent for phosphate removal, *Water*, 2021, **13**(19), 2709, DOI: 10.3390/w13192709

[21] Waghmare, C.; Ghodmare, S.; Ansari, K.; Alfaisal, F.M.; Alam, S.; Khan, M.A.; Ezaier, Y.: Adsorption of methylene blue dye onto phosphoric acid-treated pomegranate peel adsorbent: Kinetic and thermodynamic studies, *Desalin. Water Treat.*, 2024, **318**, 100406, DOI: 10.1016/j.dwt.2024.100406

[22] Gaharwar, S.S.; Majumdar, A.; Kumar, A.: Pomegranate peel-derived activated carbon: An effective adsorbent for protocatechuic acid removal and environmental remediation, *Adsorption*, 2024, **30**(8), 2219–2233, DOI: 10.1007/s10450-024-00550-y

[23] Kumar, S.; Patra, C.; Narayanasamy, S.; Rajaraman, P.V.: Performance of acid-activated water caltrop (*Trapa natans*) shell in fixed bed column for hexavalent chromium removal from simulated wastewater, *Environ. Sci. Pollut. Res.*, 2020, **27**(22), 28042–28052, DOI: 10.1007/s11356-020-09155-8

[24] Singha, B.; Das, S.K.: Biosorption of Cr(VI) ions from aqueous solutions: Kinetics, equilibrium, thermodynamics and desorption studies, *Colloids Surf. B*, 2011, **84**(1), 221–232, DOI: 10.1016/j.colsurfb.2011.01.004

[25] Dhongde, N.R., Adhikari, S.; Rajaraman, P.V.: Anticorrosion properties of ionic liquid functionalized graphene oxide epoxy composite coating on the carbon steel for CCUS environment, Environ. *Sci. Pollut. Res.*, 2025, **32**(8), 4511–4522, DOI: 10.1007/s11356-025-35984-6

[26] Dhongde, N.R.; Baranwal, P.K.; Rajaraman, P.V.: Functionalization of graphene oxide with an ionic liquid (1-butyl-3-methylimidazolium acetate): Preparation of epoxy-based coating on carbon steel for anticorrosive applications, *J. Appl. Polym. Sci.*, 2023, **140**(27), e54026, DOI: 10.1002/app.54026

[27] Baby, R.; Saifullah, B.; Hussein, M.Z.: Palm kernel shell as an effective adsorbent for the treatment of heavy metal contaminated water, *Sci. Rep.*, 2019, **9**(1), 18955, DOI: 10.1038/s41598-019-55099-6

[28] Dhongde, N.R.; Das, N.K.; Hazarika, J.; Park, J.-G.; Banerjee, T.; Rajaraman, P.V.: Azoles as corrosion inhibitors in alkaline medium for ruthenium chemical mechanical planarization applications: Electrochemical and theoretical analysis, *J. Mol. Struct*., 2025, **1320**, 139651, DOI: 10.1016/j.molstruc.2024.139651

[29] Adhikari, S.; Dhongde, N.R.; Talukdar, M.K.; Khan, S.; Rajaraman, P.V.: Investigation of carbon steels (API 5L X52 and API 5L X60) dissolution CO_2–H_2S solutions in the presence of acetic acid: Mechanistic reaction pathway and kinetics, *Arabian J. Sci. Eng.*, 2024, **49**(6), 8363–8381, DOI: 10.1007/s13369-024-08812-1

[30] Choi, J.; Wixson, T.; Worsley, A.; Dhungana, S.; Mishra, S.R.; Perez, F.; Gupta, R.K.: Pomegranate: An eco-friendly source for energy storage devices, *Surf. Coat. Technol.*, 2021, **421**, 127405, DOI: 10.1016/j.surfcoat.2021.127405

[31] Alcaraz, L.; Saquinga, D.N.; Alguacil, F.J.; Escudero, E.; López, F.A.: Application of activated carbon obtained from spent coffee ground wastes to effective terbium recovery from liquid solutions, *Metals*, 2021, **11**(4), 630, DOI: 10.3390/met11040630

[32] Meshram, S.; Thakur, C.; Soni, A.B.: Adsorption of Pb(II) form battery recycling unit effluent using granular activated carbon (GAC) and steam activated GAC, *Indian Chem. Eng.*, 2021, **63**(5), 460–477, DOI: 10.1080/00194506.2020.1795933

[33] Dong, D.; Zhao, X.; Hua, X.; Liu, J.; Gao, M.: Investigation of the potential mobility of Pb, Cd and Cr(VI) from moderately contaminated farmland soil to groundwater in Northeast, China, *J. Hazard. Mater.*, 2009, **162**(2-3), 1261–1268, DOI: 10.1016/j.jhazmat.2008.06.032

[34] Fang, W.; Jiang, X.; Luo, H.; Geng, J.: Synthesis of graphene/SiO_2@polypyrrole nanocomposites and their application for Cr(VI) removal in aqueous solution, *Chemosphere*, 2018, **197**, 594–602, DOI: 10.1016/j.chemosphere.2017.12.163

[35] Mengistie, A.A.: Adsorption of Mn(II) ions from wastewater using activated carbon obtained from Birbira (*Militia ferruginea*) leaves, *Glob. J. Sci. Front. Res.*, 2012, **12**(B1), 5–12

[36] Elewa, A.M.; Amer, A.A.; Attallah, M.F.; Gad, H.A.; Al-Ahmed, Z.A.M.; Ahmed, I.A.: Chemically activated carbon based on biomass for adsorption of Fe(III) and Mn(II) ions from aqueous solution, *Materials*, 2023, **16**(3), 1251, DOI: 10.3390/ma16031251

[37] Kwakye-Awuah, B.; Sefa-Ntiri, B.; Von-Kiti, E.; Nkrumah, I.; Williams, C.: Adsorptive removal of iron and manganese from groundwater samples in Ghana by zeolite Y synthesized from bauxite and kaolin, *Water*, 2019, **11**(9), 1912, DOI: 10.3390/w11091912

[38] Chandraker, N.; Thakur, R.S.; Chaudhari, P.K.: Removal of fluoride using bagasse activated carbon, *Desalin. Water Treat.*, 2021, **241**, 112–123, DOI: 10.5004/dwt.2021.27822

[39] Koujalagi, P.S.; Divekar, S.V.; Kulkarni, R.M.; Cuerda-Correa, E.M.: Sorption of hexavalent chromium from water and water–organic solvents onto an ion exchanger Tulsion A-23(Gel), *Desalin. Water Treat.*, 2016, **57**(50), 23965–23974, DOI: 10.1080/19443994.2016.1138329

[40] Meshram, S.; Nanewar Joshi, A.; Dharmadhikari, S.; Singh Thakur, R.: Adsorption of cadmium from water using activated carbon derived from *Ipomoea Carnea* using chemical impregnation, *IOP Conf. Ser.: Earth Environ. Sci.*, 2020, **597**, 012005, DOI: 10.1088/1755-1315/597/1/012005

[41] Ho, Y.S.; McKay, G.: Pseudo-second order model for sorption processes, *Process Biochem.*, 1999, **34**(5), 451–465, DOI: 10.1016/S0032-9592(98)00112-5

[42] Weber, W.J.; Morris, J.C.: Kinetics of adsorption on carbon from solution, *J. Sanit. Eng. Div.*, 1963, **89**(2), 31–59, DOI: 10.1061/JSEDAI.0000430